Research Article

Identification of Stage-Specific Breast Markers using Quantitative Proteomics

Sadr-ul-Shaheed[a], Nitin Rustogi[a], Andrew Scally[b], Julie Wilson[c], Helene Thygesen[d], Maria A. Loizidou[e], Andreas Hadjisavvas[e], Andrew Hanby[d], Valerie Speirs[d], Paul Loadman[a], Richard Linforth[f], Kyriacos Kyriacou[e]*, Chris W. Sutton[a]*

[a] Institute of Cancer Therapeutics, University of Bradford, UK

[b] School of Health Studies, University of Bradford, UK

[c] York Centre for Complex Systems Analysis, University of York, UK

[d] Leeds Institute of Cancer and Pathology, Leeds, UK

[e] The Cyprus Institute of Neurology and Genetics, Nicosia, Cyprus

[f] Bradford Royal Infirmary, Bradford, UK

*Correspondence to Dr. Chris Sutton, Institute of Cancer Therapeutics, University of Bradford, Tumbling Hill Street, Bradford, West Yorkshire, BD7 1DP, UK, t. +44 1274 236480, f. +44 1274 233234, e. c.w.sutton@bradford.ac.uk, and Dr. Kyriacos Kyriacou, The Cyprus Institute of Neurology and Genetics, 6, International Airport Avenue, Agios Dometios 2370, P.O. Box 23462 / 1683, Nicosia, Cyprus, t. +357 22392631, f. +357 22392641, e. kyriacos@cing.ac.cy

Keywords: breast cancer, invasive carcinoma, DCIS, fibroadenoma, proteomics, iTRAQ, mass spectrometry, tissue microarray, western blotting

Abbreviations: CHCA, α-cyano-4-hydroxy-cinnamic acid; CING, The Cyprus Institute of Neurology and Genetics; DCIS, ductal carcinoma *in situ*; ER, estrogen receptor; L/N lymph node metastasis; pt., patient; PR, progesterone receptor; SC, sequence coverage; S.D., standard deviation; TBS, Tris-buffered saline; TEAB, triethylammonium bicarbonate

Abstract

Matched healthy and diseased tissues from breast cancer patients were analysed by quantitative proteomics. By comparing proteomic profiles of fibroadenoma (benign tumors, 3 patients), DCIS (non-invasive cancer, 3 patients) and invasive ductal carcinoma (4 patients) we identified protein alterations which correlated with breast cancer progression. Three 8-plex iTRAQ experiments generated an average of 826 proteins identifications, of which 402 were common. After excluding those originating from blood, 59 proteins were significantly changed in tumor compared to normal tissues with the majority associated with invasive carcinomas. Bioinformatics analysis identified relationships between proteins in this subset including roles in redox regulation, lipid transport, protein folding and proteasomal degradation, with a substantial number increased in expression due to Myc oncogene activation. Three target proteins, cofilin-1 and p23 (increased in invasive carcinoma) and membrane copper amine oxidase 3 (decreased in invasive carcinoma), were subject to further validation. All three were observed in phenotype-specific breast cancer cell lines, normal (non-transformed) breast cell lines and primary breast epithelial cells by Western blotting, but only cofilin-1 and p23 were detected by multiple reaction monitoring mass spectrometry analysis. All three proteins were detected by both analytical approaches in matched tissue biopsies emulating the response observed with proteomics analysis. Tissue microarray analysis (361 patients) indicated cofilin-1 staining positively correlating with tumor grade and p23 staining with ER positive status, both therefore merit further investigation as potential biomarkers.

Introduction

Breast cancer is the most common cancer in women and the second most common of all types. Through the application of surgery, radiotherapy, chemotherapy, the development of targeted immune and hormone-based therapies and combined treatment, the 5 year survival rate has increased from 50% in the 1970's to currently 80%. Indeed, almost two thirds of women are living more than 20 years after treatment. Despite this, 458,000 women died of breast cancer in 2008 and it is the most frequent cause of cancer-related death in women in developing regions and numbers in developed countries equal those caused by lung cancer. The incidence of breast cancer is highest in Western Europe (increasing by 11% in women under 50 between 1993- 95 and 2008- 10) and continues to rise in most developed countries[1]. Furthermore, the number of breast cancer-related deaths in women under 50 has reached all time highs in United Kingdom in 2010 (http://www.cancerresearchuk.org/cancer-info). Changes in lifestyle are contributing significantly to increased prevalence, such as escalating alcohol consumption, oral contraception, reproductive behavior, hormone replacement therapy and postmenopausal obesity, all identified as factors associated with causing breast cancer[2]. Consequently, and despite the progress made to date in treating the disease, the constant changing dynamics of breast cancer incidence requires continuous investigation to identify new methods of detection and treatment.

Extensive research has revealed breast cancer to be a diverse and complex disease that can be classified by histopathological morphology, disease progression, tumor size and stage, lymph node status and molecular phenotype. Molecular classification of breast cancer defined 5 main different phenotypes[3], which have contributed significantly towards targeted therapy. With the continuing expansion of the breast cancer genome and transcriptome[4], further stratification towards personalised treatment can be anticipated. This has been invaluable in defining treatment regimens and predicting outcome or responsiveness.

Histopathological investigation of breast carcinoma delineates two main groups – ductal carcinoma of no specific type (NST) and lobular carcinoma, with a number of less common types[5]. Histological features, supported by mammography, can also determine disease progression, through well characterised stages that may include benign atypical ductal hyperplasia (ADH), localised pre-invasive ductal carcinoma in situ (DCIS) or lobular carcinoma in site (LCIS), to the more advanced stages of invasive ductal carcinoma or invasive lobular carcinoma, which spread into the surrounding breast tissue. In addition, younger women in particular, may develop fibroadenomas, comprising benign fibrous lumps, which do not seem to develop into cancerous growth.

The transition of breast tissue from a benign state to an invasive state capable of uncontrolled proliferation is not well understood. Not all DCIS become cancerous and, for those that do, the molecular and/or temporal triggers are not known. Only 25 to 50% of DCIS will progress to invasive carcinomas if left untreated[6] and currently it is not possible for the pathologist or clinician to predict which will advance to a more aggressive stage. Treatment options for DCIS include total mastectomy, local excision (LE) plus adjuvant radiotherapy (RT), or LE alone, but these treatments in many cases prove superfluous and may cause unnecessary side effects, which compromise the quality of patient's lives.

Biomarkers that offer the possibility of detecting the early onset of disease progression or can differentiate between those tumors that remain dormant and those that that will develop into aggressive invasive malignancies would provide opportunities for an earlier as well as a more targeted intervention, avoiding unnecessary costly treatments and improving survival. Proteomics has been used previously to identify early biomarkers, but none have so far progressed to clinical validation. Building on a preliminary study[7], we have used an iTRAQ proteomics strategy to compare matched normal and tumor tissues from Cypriot patients with fibroadenoma (benign), DCIS (pre-invasive) and invasive ductal carcinoma (malignant). In Cyprus, a successful population-wide breast cancer screening programme was

initiated in 2003 according to EU guidelines. Within Europe, Cyprus has the lowest mortality rate for all cancers, except for breast cancer, which is closer to the average, however it is not known if this is related to treatment, genetics or some other factor. Our objective is to identify proteins whose expression correlates with cancer progression and validate candidates by Western blotting, multiple reaction monitoring mass spectrometry (MRM MS) and tissue microarray as possible markers for early detection of breast cancer.

Materials and Methods

Patient characteristics and tissue procurement. The CING study protocol and patient consent forms were approved by the Cyprus National Bioethics Committee. Patients underwent surgery for removal of breast lesions and subsequent histopathological diagnosis. Following inspection by a histopathologist, resected specimens were snap frozen in isopentane cooled by liquid nitrogen and stored at -80^{o}C. Tissues from the breast lesion and areas identified as normal, at least 5 cm apart, were obtained. Biopsies from patients with fibroadenoma, DCIS or invasive ductal carcinoma were selected for proteomic analysis. Frozen sections were cut from matched blocks of normal and disease breast tissue using a Bight's cryostat as described previously[7]. Three 8-plex iTRAQ experiments (A, B and C) were performed, each with matched normal and disease cryosections from 10 patients (Table 1). One fibroadenoma biopsy (patient 1), was used in all three experiments for inter-experiment evaluation. Tissue microarray (TMA) samples were prepared from archival tissue blocks and clinicopathological data were obtained from the Leeds Breast Tissue Bank for patients diagnosed with breast cancer cases at the Leeds Teaching Hospitals Trust from 1994 to 1997. Ethical approval was given by Leeds (East) Research Ethic Committee, reference 06/Q1206/180. Primary breast cells were isolated from biopsy material collected from a patient undergoing double mastectomy for BRCA1 risk reduction at Bradford Royal Infirmary and determined by pathology to be essentially normal. Ethical approval was given by Leeds (East) Research Ethic Committee, reference 07/H1306/98+5.

Cell lines culture conditions. Cancer cell lines were obtained from American Type Culture Collection (Manassas, VA) and maintained in RPMI medium containing 10% v/v foetal calf serum (FCS). HB2 normal breast cell line was grown on DMEM + Glutamax-1 (Gibco® Life Technologies, Paisley, UK) containing 10% FCS supplemented with hydrocortisone (5 µg/ml) and insulin (10 µg/ml), and MCF-10A normal breast cells were cultured in MEGM Bullet Kit (Lonza Walkersville, Inc USA), referred to as standard growth medium.

Protein extraction from cell lines and primary epithelial cells. Cells were harvested by trypsin treatment on reaching 90% confluence. Cells were washed three times with PBS to remove residual FCS, each time the supernatant decanted and discarded after centrifugation at 1,000 rpm for 5 minutes, and the resulting pellet stored at -20^{o}C until required. Pellets equivalent 5 x 10^{6} cells were thawed, 100μl of urea extraction buffer (7M urea, 2M thiourea, 4% w/v CHAPS, 50mM DTT in PBS pH7.4 containing protease inhibitor cocktail [Roche diagnostics GmbH, Germany]) added, vortexed, sonicated and then centrifuged. The protein concentration of each cell line extract was measured using the Bradford assay (Bio-Rad Laboratories, Hemel Hempstead, UK)[8] and then stored as 10μl aliquots at -20^{o}C.

Protein extraction from tissues by solubilisation and sonication. The following proteomics methods were applied to each of the three iTRAQ experiment (workflow schematic in Supplementary Figure 1).

Protein extracts were prepared in parallel from matched normal and diseased tissues for four patients using a dual lysis buffer[7]. In brief, for each sample (10 cryosections), RIPA lysis buffer (50 μl, PBS pH 7.4, 0.1% w/v SDS, 0.25% w/v sodium deoxycholate containing EDTA-free protease inhibitor cocktail) was added, subjected to vortexing for 30 minutes at room temperature and sonicated for 20 seconds on ice using a Status US70 sonicating probe (Philips Harris Scientific, UK). The samples were centrifuged at 13,400 rpm for 20 minutes, 4^{o}C and the liquid phase extracted to new tubes. Urea lysis buffer (50 μl, 7M urea, 2M thiourea, 4% w/v CHAPS, 50mM DTT in PBS containing EDTA-free protease inhibitor cocktail) was added to the pellet two times, each time treated with vortexing, sonication and centrifugation, and the resulting supernatant combined with the RIPA buffer protein extract. The protein concentration of each total extract for each patient matched normal and tumor biopsy was measured using the Bradford assay and stored at -20^{o}C.

Proteomics sample preparation and mass spectrometry analysis. Each protein extract (50 μg of protein) was precipitated overnight with 100% acetone at -20^{o}C, centrifuged for 20 minutes at 13,400

rpm at 4^{o}C and the pellet resuspended in 1M TEAB (Sigma-Aldrich, Poole, UK), 0.1% w/v SDS. Each protein sample was reduced with 50 mM DTT for 15 minutes at 60^{o}C, alkylated with 100 mM IAA at ambient temperature for 15 minutes and digested with 2 μl of a 1mg/ml solution of modified sequencing grade trypsin (Roche Diagnostics GmbH, Germany) at 28^{o}C for 18 hours. After digestion, each sample was lyophilised, resuspended in TEAB, 0.1% SDS and an iTRAQ reagent (AB Sciex UK Limited, Warrington, UK) added as outlined in Table 1, for 2 hours at room temperature. The labelled peptides were then combined together, desalted on an Isolute C18 RP LC column (Kinesis Ltd., St. Neots, UK) and the eluate lyophilised. The total iTRAQ-labelled peptide sample was resuspended in OffGel peptide sample buffer (containing pH 3-10 ampholytes) and applied to an OffGel 3100 (Agilent Technologies, Wokingham, UK) IEF system, using a pH 3-10 high resolution strip, for 50kV hours. Twenty-four fractions were collected, desalted on Isolute C18 RP cartridges and then lyophilised.

LC MALDI. OffGel fractions were analysed on an LC Packings UltiMate 3000 capillary HPLC system (Dionex, Camberley, Surrey, UK). Lyophilised fractions were resuspended in 6.5 μl of 2% acetonitrile, 0.05% TFA (mobile phase A), injected and washed on a C_{18}, 300μm x 5mm, 5μm diameter, 100Å PepMap pre-column (LC Packings, Sunnyvale, CA) before transfer to a C_{18}, 75μm x 15cm, 3μm diameter, 100Å PepMap column (LC Packings) and elution of peptides with a linear gradient to 10% to 40% mobile phase B (80% acetonitrile, 0.05% TFA) over 105 minutes. A total of 384, 75 nl fractions were co-deposited with 1.2 μl of a saturated CHCA matrix (Bruker Daltonik GmbH, Bremen, Germany) solution onto a MTP AnchorChip 800/384 target plate (Bruker Daltonik) using a Proteineer FC fraction collector (Bruker Daltonik) and allowed to air-dry. Peptide Calibration Standard II (Angiotensin I, Angiotensin II, Substance P, Bombesin, ACTH clip 1-17, ACTH clip 18-39, Somatostatin 28, Bradykinin fragment 1-7 and Renin Substrate Tetradecapeptide porcine; covering the mass range 700 Da – 3200 Da, Bruker Daltonik) was applied between each group of 4 fractions. Mass spectrometric analysis was carried out using a MALDI-TOF/TOF UltraFlex II instrument (Bruker Daltonik), using a 200 Hz smartbeam laser (>250

μJ/pulse) in reflector mode. A fully automated workflow was performed using WarpLC software (version 1.2), which encompassed data acquisition (FlexControl v3.0), data-processing (FlexAnalysis v3.0 - TopHat baseline subtraction, Savitzky-Golay smoothing and SNAP peak detection algorithms), compilation of a non-redundant list of peptides from the 384 HPLC fractions, data-dependent MS/MS of each peptide using LIFT mode, compilation of the MS/MS fragment mass lists into a batch (WarpLC v1.3). Where there was sufficient sample, replicate LC MALDI analyses were performed for each OffGel fraction.

Database searching. MS/MS fragment mass lists were searched, via Proteinscape v3.0, (Bruker Daltonik), using Mascot software version 2.4 (Matrix Science, UK)[9] against Swiss-Prot version 2011_12 containing 20,323 human protein sequences with search parameters: trypsin digestion, 2 missed cleavage, variable modification of methionine oxidation, fixed modifications of cysteine (carbamidomethylation) and iTRAQ (lysine and N-termini), and a 95% confidence interval threshold ($p<0.05$, Mascot score ≥ 29). A decoy search (based on automatically generated random sequences of the same length) was employed to determine the rate of false-positive identifications. For MALDI MS/MS data with a precursor mass tolerance of 100 ppm and fragment-ion mass tolerance of 0.7Da, the false discovery rate at the identity threshold was an average of 1.82% (S.D. = 1.58%) for 127 LC MALDI runs from all three experiments. iTRAQ labelling efficiency was determined by searching MS/MS data using iTRAQ as a variable modification, performing a survey of 400 peptides of labelled and non-labelled peptides ($p<0.05$, Mascot score ≥ 29) in the twenty highest scoring proteins from individual LC MALDI experiments and calculated to be 96.2%, 98.1% and 98.3% for experiments A, B and C respectively.

Data processing. Non-redundant protein profiles for each Experiment were created in Proteinscape by combining the corresponding LC MALDI datasets. Qualitative (at least one ranked first peptide, Mascot score ≥20) and quantitative filters (at least two iTRAQ tumor:normal ratios) were used to define each dataset. The three datasets were further consolidated to a single list of proteins common

to all the experiments, each with 12 iTRAQ ratios representative of the 10 patients (one individual analysed three times for inter-experimental evaluation).

Statistical analysis was undertaken using Strata software (Release 9.2). In order to compare patient-to-patient protein profiles, the iTRAQ tumor:normal ratios for each protein, for each patient were normalised to an average of 1.0. Therefore, tumor:normal ratios with values > 1 signify higher levels in tumor compare to normal tissue and tumor:normal ratios with values < 1 represent higher levels in normal compare to tumor tissue. The upper and lower 5^{th}, 10^{th} and 25^{th} percentile protein populations of the normalised ratios were calculated for each patient. Proteins were then organised based on the average iTRAQ ratio for the four invasive carcinoma patients, so that those proteins that were most significantly changed in each disease state could be identified. The iTRAQ ratios were used as variables in Principal Component Analysis (PCA) (R Project for Statistical Computing http://www.r-project.org/) to correlate protein profiles with stages of the disease.

Protein-protein interactions and network associations for significantly changed components were performed using STRING (version 9.05, http://string-db.org/) and Ingenuity Interactive Pathway Analysis software (2013 version) respectively.

Western blot analysis. Protein extracts were prepared from cell lines or from cryosections independent of those used for proteomics analysis. Patient samples, equivalent to 30μg of protein, were mixed with 10μl of SDS reducing buffer (for cell lines, 20μg of protein was used with 5μl of SDS reducing buffer), heated to 60^{o}C for 15 minutes and on cooling applied to SDS polyacrylamide gels, with a 4% (v/v) stacking gel and 12% (v/v) separating gel in a SDS-PAGE (Laemmli) buffer system. Gels were run on a Mini-PROTEAN® 3 Cell system (Bio-Rad, Hemel Hempstead, UK) for 10 minutes at 80V and then 60 minutes for 150V. Proteins were transferred to a nitrocellulose membrane by electroblotting for 2 hours at 85mA in a Mini Trans-Blot® Cell (Bio-Rad, Hemel Hempstead, UK). The blotted membrane was incubated in blocking buffer (5% w/v skimmed milk in Tris-buffered saline, 0.05% v/v Tween), then with

the appropriate primary antibody (anti-cofilin-1 rabbit polyclonal antibody, Abcam, Cambridge, UK, 1 in 2000 dilution, anti-p23 mouse [JJ3] monoclonal antibody, Abcam, 1in 1000 dilution, anti-AOC3 mouse [Clone 393112] monoclonal antibody, R&D Systems, Minneapolis, US, 1 in 500 dilution, or anti-beta-actin, mouse monoclonal antibody, Sigma, Dorset, UK, 1 in 5000 dilution) in blocking buffer was incubated overnight at 4^{o}C. After removal of the primary antibody with three TBS-Tween buffer washes, the appropriate secondary antibody (anti-rabbit IgG-conjugated with horseradish peroxidise, Dako, Glostrup, Denmark, 1 in 3,500 dilution or anti-mouse IgG-conjugated with horseradish peroxidise, Abcam, 1 in 3,500 dilution), in blocking buffer, was incubated with the membrane for 45 minutes at room temperature. The residual secondary antibody was removed with three TBS-Tween washes and proteins detected by addition ECL Plus Western Blotting reagent then exposed to X-ray film (GE Healthcare, Amersham, UK).

Multiple reaction monitoring mass spectrometry (MRM MS). MRM MS was performed on a Waters Quattro Ultima triple quadruple mass spectrometer with on-line Waters Alliance 2695 HPLC Separation system and 996 Diode array Detector. A two-stage HPLC gradient using solvent A (90% water, 10% methanol, 0.1% formic acid) and solvent B (80% methanol, 20% water, 0.1% formic acid) on a Luna C_{18} column (2 mm ID x 25 cm length, 5μm particle size, Phenomenex Inc., Macclesfield, UK) was used for separation of the target peptides. A linear gradient of 20 to 80% % solvent B was applied for 70 minutes followed by a column wash for 20 minutes using 10% solvent B. The HPLC retention time, cone voltage and collision energy were optimised using synthetic proteotypic peptides for cofilin-1 (LGGSAVISLEGKPL, EILVGDVGQTVDDPYATFVK and YALYDATYETK), p23 (DVNVNFEK) and AOC3 (YQLAVTQR, EALAIVFFGR and SPVPPGPAPPLQFYPQGPR) (Supplementary Table 1). Calibration curves were prepared with the synthetic peptides (Supplementary Figure 2) before quantitative analysis of trypsin digests of fresh protein extracts from cell lines (amol/cell) and patient biopsies (amol/mg tissue).

Tissue microarray (TMA) analysis. Sections were prepared from 361 cases of breast cancer represented on TMAs as described previously[10]. In parallel TMA sections, antibodies to cofilin-1 (anti-cofilin-1 rabbit polyclonal antibody, 1/5000 dilution, Abcam, Cambridge, UK,) or p23 (anti-p23 rabbit polyclonal antibody, 1/24000 dilution, Sigma, Dorset, UK) were applied for 1 hour at room temperature. Slides were washed with PBS before incubation with horse radish peroxidise (HRP)-conjugated secondary antibody (Santa Cruz Biotechnologies, Heidelberg, Germany) at room temperature for 40 minutes. Visualisation of bound antibodies was performed using diaminobenzidine (En-vision, Dako, Ely, UK), followed by haematoxylin counterstaining, dehydration and mounting with cover slips. Immunohistochemistry for cofilin-1 was evaluated by SuS, supervised by AMH, using an adapted Allred scoring scheme previously described for estrogen receptor[11], i.e. the proportion of cell stained (0 = no cells stained, 1= 1%, 2 = 1-10%, 3 = 10-33%, 4 = 34-66% and 5 = 67-100%) and the intensity of staining (0 = negative, 1 = weak, 2 = moderate and 3 = strong). The intensity staining score of 0-1 was interpreted as the absence and score of 2-3 as the presence of cofilin-1 in the tissue. p23 IHC was assessed according to the system described previously[12], which scored cytoplasmic (0 = no cytoplasmic staining, 1+= weak staining, 2+ =intermediate staining 3+ = strong staining) and nuclear (0 = no positive nuclei, 1+= weak staining, 2+ =intermediate staining 3+ = strong staining) staining independently. Statistical analysis was performed using PRISM 5.0 software (GraphPad Software Inc., San Diego, California, USA).

Results and Discussion

Proteomics analysis. Three iTRAQ experiments were performed for the proteomic analysis of matched normal and diseased tissues from 10 patients with benign pathologies or breast cancer. Histopathology results categorised the tumors into fibroadenoma, DCIS and invasive ductal carcinoma. With the exception of one fibroadenoma biopsy (patient 1), which was prepared in triplicate and used in each of the three experiments for inter-experiment variation, sets of patients samples were selected randomly (Table 1). Following filtering to remove proteins detected only by single peptides or no iTRAQ data, 874 proteins (4,812 total peptides) were identified in experiment A, 790 proteins (4,361 peptides) in experiment B and 814 proteins (4,768 peptides) in experiment C. A non-redundant list of 1406 proteins was prepared, of which 402 proteins were detected in all three experiments (Figure 1A), each constituent therefore imparting quantitative data in the form of iTRAQ ratios for each patient (Supplementary Table 2).

Each protein iTRAQ ratio for each patient was normalised, using the average peptide iTRAQ ratio, so that a heat map was created that enabled comparison of specific protein changes between each patient and across disease states (Figure 1B). PCA analysis of the tumor:normal ratio values for each patient clustered datasets broadly by disease state (Supplementary Figure 3). The separation between patients with invasive carcinoma and other stages can be seen along the first principal component (pc1), which accounts for 31% of the variance in the data. In two dimensions, there is no distinction between patients with fibroadenoma and those with DCIS, though samples from patient 1 appear to cluster separately, but consistently, across the three experiments. The dispersion of invasive carcinoma patients reflected variations in individual protein ratios, but showed clear differences from the fibroadenoma and DCIS groups. Examination of the loadings indicated that proteins cofilin-1, p23, 60S ribosomal protein L24, cysteine-rich protein 1 and cysteine and glycine-rich protein 1 were most

responsible for the variance along pc1. All have high values for the ratios, indicating increased expression levels in tumor tissue.

The proteins common to all three experiments were subject to statistical analysis to identify those that were significantly increased or decreased in tumor compared to normal for each patient. The upper and lower 5%, 10% and 25%-ile groups of proteins were determined for each patient. The frequency with which each protein appeared in a percentile cluster was recorded to identify those that were associated with each disease state. Greater significance was given to those proteins that occurred with the same frequency but in a lower percentile group (5%>10%>25%). Hence, significant proteins were defined as those with tumor-to-normal ratios in the upper or lower 5% or 10% of the total (402 common proteins), for ≥3 of 5 fibroadenoma, ≥2 of 3 DCIS or ≥3 of 4 invasive carcinoma patients and in the upper or lower 25% for ≥4 of 5 fibroadenoma, 3 of 3 DCIS or 4 of 4 invasive carcinoma patients. Previously, we had segregated proteins based on their predominant localisation – intracellular, extracellular or blood-based[7]. However, in the present study all 402 proteins were analysed together. Gene Ontology based localisation was applied, identifying proteins as intracellular (64%), membrane-bound (5%), extracellular (stromal) (13%) or serum/blood-based (18%). Of 69 proteins that were decreased in at least three of four invasive carcinomas compared to the equivalent normal tissue, 39 originated from serum (for example, immunoglobulins, globins, lipoproteins, transport proteins and complement factors). These proteins were most likely lower due to the gross decrease in vasculature, and consequently lower blood content, in tumors compared to normal breast tissue, and therefore excluded from further consideration. This left 59 proteins that were significantly increased or decreased (Table 2).

In a previous study of matched normal and tumor tissues from six patients, by 2D gel electrophoresis and MS analysis, 315 proteins were identified of which 57 were differentially expressed in individual cases including cofilin-1, profilin, peroxiredoxin 1, heterogeneous nuclear ribonucleoprotein

A2/B1 which were also increased in our study[13]. Proteomic profiling of normal and infiltrating ductal carcinomas from 10 Tunisian patients, using non-equilibrium pH gradient electrophoresis and MALDI MS peptide fingerprinting identified 20 proteins that were significantly changed[14]. As with our results, immunoglobulin G was observed to be decreased and peptidyl prolyl isomerase A, cofilin-1, heterogeneous nuclear ribonucleoprotein A2/B1, and phosphoglycerate kinase 1 were increased. Other proteins that we identified with significantly altered levels have also been shown by others to be differentially expressed in breast cancer models. These include cytokeratin-15[15], cytokeratin-19[16], cytokeratin-18[17], cytokeratin-8[17-18], prolactin-inducible protein[19, 20], calreticulin[21, 22], small breast epithelial mucin[23, 24], peptidyl-prolyl cis-trans isomerase A[25], p23[12, 26, 27], transcription intermediary factor 1-beta[28], glyceraldehyde-3-phosphate dehydrogenase[29], triosephosphate isomerase[25], protein disulfide-isomerase A3[22], protein disulfide-isomerase[30] and tropomyosin alpha-3 chain[22], which were all increased, and alpha-1-acid glycoprotein 1[20], caveolin-1[10, 31], adipocyte fatty acid-binding protein[32, 33], perilipin[34] and polymerase I and transcript release factor[35] were all decreased.

STRING analysis emphasised that the majority of the differentially expressed subset of 59 proteins interact within established complexes or functional relationships (Figure 2). IPA Upstream regulator analysis provided evidence of 13 genes exhibiting a response associated with Myc oncogene activation (up-regulated – TPI1, PPIA, HSPE1, HNRPD, HMGN2, EEF2, DBI, CRIP1, COX6B1 and down-regulated – SUCLA2, CRYAB, COL4A1, CAV1) ($p<5.05E-09$), four genes with Ca+binding protein S100P activation (up-regulated – CFL1, KRT19, KRT8 and KRT18) ($p<7.19E-09$) and seven with folate receptor 1 activation (regulation of GLRX, TPI1, PFN1, CAV1, LAMB2, CAT, and AOC3)($p<8.39E-09$)(Supplementary Figure 4). Myc, S100P and folate receptor 1 over expression or malfunction have been associated with breast cancer progression[36,37,38]. Key networks correlating with the identified proteins were associated with cell morphology, cellular assembly and organisation, free radical scavenging and cell-to-cell signalling (Supplementary Figures 5a-c). Reduced levels of extracellular superoxide dismutase and

membrane-bound copper amine oxidase, both of which produce hydrogen peroxide would results in lower levels of toxic reactive oxygen species (ROS) in the interstitial fluid surrounding the cancer cells, thereby improving the proliferative milieu. Increased expression of peroxiredoxin-1 and -5, along with redox regulating proteins, glutaredoxin-1 and thioredoxin, would succeed in reducing intracellular ROS levels and further enhance the environment for growth. Catalase, which would also neutralise hydrogen peroxide and exhibited reduced levels, may reflect a more complex expression profile as it is expressed in erythrocytes, which like other blood proteins observed in our results, is extensively decreased in tumor compared to normal tissues.

A group of lipid transport and metabolism proteins (fatty acid binding protein 4, hormone sensitive lipase, perilipin, carboxylesterase 1, EH domain-containing protein 2, caveolin-1, polymerase I and transcript release factor) were decreased in tumor compared to normal tissues. This may simply reflect their predominant expression in adipocytes which were substantially reduced in tumor. However, the diminished levels of caveolin-1 may also relate to its role in tumor suppression, which as a consequence would result in cancer progression. Loss of caveolin-1 in cancer-associated fibroblasts has previously been shown to correlate with poor prognosis in breast cancer[10], but increased expression has also been linked with metastasis and anti-cancer drug resistance[39].

TRIM28, is a multi-functional E3 SUMO-protein ligase, increased in tumor compared to normal, which ubiquitinates p53, leading to its proteasomal degradation, thereby removing a tumor suppressor and preventing apoptosis. Network analysis suggested that, through ubiquitination, TRIM28 may control the activity of other identified up-regulated proteins, including small acidic protein, cysteine-rich protein 1, SH3 domain-binding glutamic acid-rich-like protein, cytochrome c oxidase subunit VIb isoform 1, 60S ribosomal protein L24, elongation factor 1-delta, histone H2A type 1-H and glucosidase 2 subunit beta.

Three proteins, cofilin-1, p23 and AOC3, were selected to validate the proteomics approach undertaken. Cofilin-1 was an example of a protein identified with high confidence (20 peptides, 105

spectra, average Mascot score of 462 and 84.3% sequence coverage across the three experiments) as increased in tumor compared to normal tissue (average iTRAQ ratio of 1.836 for four invasive carcinoma measurements) and highlighted by PCA as significantly contributing to the invasive carcinoma signature. p23, also increased in tumor compared to normal tissue, is a protein detected with low confidence (3 peptides, 6 spectra, average score = 31, 18.8% sequence coverage and average iTRAQ ratio of 2.161, but also strongly associated by PCA with the invasive carcinoma signature), therefore requiring verification by alternative methods. AOC3 was an example of a protein identified with confidence and decreased in tumor compared to normal tissues (11 peptides, 56 spectra, average score = 272, 16.4% sequence coverage and average iTRAQ ratio of 0.308).

Cofilin-1 plays a pivotal role in directing actin polymerisation into filaments that form lamellipodia, then invadopodia, to push the membrane envelope of metastatic cells on the first steps towards cell motility and invasion[40]. It has been shown to be over-expressed in other cancer tissues, in addition to breast tumors[13-14], using immunohistochemistry (esophageal squamous cell carcinoma[41], gall bladder squamous cell and adenosquamous carcinomas[42], ovarian[43, 44], non-small cell lung cancer[45 46]) and 2D gel electrophoresis with MS identification (oral squamous[47], prostate[48], renal[49]). p23 is a multifunctional protein that modulates the activity of aryl hydrocarbon receptor and, in conjunction with HSP90, increases the affinity of steroid hormone receptors for their respective ligands[12, 50, 51]. It is also involved in the recruitment of steroid receptors and telomerase to the nucleus where they regulate transcriptional expression of target genes[52], it stabilises specific kinases and has glutathione-dependent cytoplasmic prostaglandin E synthase 3 enzyme activity[53]. The role of p23 in breast cancer has also been described, with over-expression enhancing ER-dependent transcriptional events including promoting transition from non-invasive to invasive cells through activation of metastasis-related genes and has been established as a potential target to prevent development of secondary tumors. AOC3 is a membrane protein up-regulated in adipocyte differentiation and therefore expected to be reduced in

tumor tissue where adipocyte composition is lower than normal tissues. Amino oxidases have been shown to inhibit tumor growth. The decreased levels of AOC3 observed in our proteomics analysis may be associated with removal of a repressive factor which consequentially enables tumor growth[54] and therefore warrants further investigation.

Western blot analysis of cofilin-1, p23 and AOC3 was performed on protein extracts from breast cancer cell lines and tissues. Cell lines representative of five breast cancer phenotypes (Luminal A, Luminal B, basal-like, Claudin-low and HER2), normal breast cell lines and normal primary breast epithelial cells were analysed for expression profile screening (Supplementary Figure 6A and B). Cofilin-1 was ubiquitously expressed in all cell lines tested with a single band at molecular weight of 21.0 kDa (theoretical molecular weight = 18.5 kDa), p23 was observed as a double band with the weaker, sporadic band A at 22.6 kDa and stronger band B at 20.5 kDa (expected molecular weight from sequence = 18.7 kDa) in breast cancer cell lines, normal breast cell lines and primary epithelial cells. AOC3 was also generally well expressed across all the cell lines despite normally being associated with adipocytes, but was much weaker in normal cell lines compared to cancer cell lines. A main band of 132.0 kDa and weaker band of 87.9 kDa (expected molecular weight = 84.6 kDa) were detected. As AOC3 has 6 N-linked and 1 O-linked glycosylation sites, a higher molecular weight than that calculated from the amino acid sequence was expected on SDS PAGE.

Matched tissues from patients with invasive carcinoma indicated the presence of cofilin-1 in the tumor samples and either lower or complete absence of the protein in the equivalent normal tissues by Western blot analysis (Figure 3A). As with cell line analysis, p23 was observed as two bands, with band B stronger than band A, and the former observed to be differentially expressed between tumor and normal tissues. Also, in support of the proteomics results, AOC3 was detected in most normal samples, but absent from tumors (Figure 3A). Cofilin-1 was also analysed in matched normal and diseased tissues

from fibroadenoma and DCIS patients. In both cases, cofilin-1 levels were either unchanged or marginally increased in tumors compared to the equivalent normal sample (Figure 3B).

MRM MS was performed using proteotypic peptides for cofilin-1 (analysis of three unique peptides), p23 (one peptide) and AOC3 (three peptides). Calibration curves were prepared using synthetic peptides, each of which exhibited a linear response over 3 orders of magnitude in the range of 10ng/ml to 10μg/ml (Supplementary Figure 2). Cofilin-1 and p23, but not AOC3, were detected in all cell lines. MRM MS analysis confirmed the ubiquitous presence of cofilin-1 in the range of concentrations of 360 (MCF7, luminal A) to 860 (BT474, luminal B) amol/cell (average of 3 measurements for each peptide for each cell line) for cancer cell lines, but lower levels for normal cell lines 67-73 amol/cell (Supplementary Figure 7A). Somewhat surprisingly, cofilin-1 levels were low in MDA-MB-468 cells (383 amol/cell), which are derived from an aggressively invasive basal-like tumor. This could be due the cells down-regulating cofilin-1 expression once they have achieved an invasive status or due to phenotypic changes resulting from cell line immortalisation. Similar to cofilin-1, p23 was detected in all, ranging from 11 (Hs578-T, Claudin-low) to 60 (MDA-MB-453, HER2+) amol/cell (average of 2 measurements for one peptide) for cancer cell lines and lower levels for normal cells – 4 to 7 amol/cell (Supplementary Figure 7B).

MRM MS analysis of cofilin-1, p23 and AOC3 was performed on fresh trypsin digests of protein extracts from matched biopsies of 5 invasive carcinoma, 1 DCIS and 1 fibroadenoma patients. The results corroborated previous observations with significantly higher levels of cofilin-1 and p23 in tumor than normal for invasive carcinoma patients, and the reverse for AOC3 (Figure 4). Similarly, there was little or no change in the levels of the proteins in fibroadenoma or DCIS patients. The 3 peptides selected for AOC3 were from different regions of the protein sequence to allow for post-translational truncation. The MRM MS results indicated that only one of the peptides (YQLAVTQR) was detected in breast cancer tissues and none in the cell lines. Western blot results of AOC3, using an antibody generated to the

recombinant protein (Gly27-Asn763) indicated that the protein was essentially intact in cell lines and breast tissues. The most likely explanation for the discrepancy is that the levels of AOC3 were much lower in epithelial cell lines and consequently not observed above the limit of detection by MRM MS, compared to the amounts present in adipocyte-rich normal tissues or detected in Western blots.

TMAs of 361 breast cancers were prepared for cofilin-1 and p23 (representative images are shown in Supplementary Figure 8). Cofilin-1 was scored based on the proportion of cancer cells stained and intensity of intracellular cofilin-1 staining as a measure of expression. Of the arrays, 81% stained positively for cofilin-1. Intensity of staining correlated with proportion of cells stained and was positively associated with tumor grade and tumor type (invasive ductal and invasive lobular) (Table 3A). p23 staining was differentiated into nuclear and cytoplasmic sub-cellular localisation. In agreement with Simpson *et al*[12], strong cytoplasmic staining also correlated with strong nuclear staining (Table 3B). Like cofilin-1, p23 correlated positively with invasive ductal and invasive lobular carcinoma, but also with ER expression status.

Conclusions

There has been extensive research to discover biomarkers to provide clinicians with accurate information that will support the best outcome for the patient, whether this is for early detection, selection of therapy, or to predict responsiveness or resistance to treatment. Our objective is to identify proteins that correlated with breast tumor progression, starting from benign through to malignant states. We elected to use breast tissue biopsies as the most direct source associated with the disease and generated samples that comprised proteins from the various constituent epithelial, fibroblast, myo-epithelial cell types, stroma, lymphatic system and vasculature. Quantitative proteomics revealed a set of proteins that were increased or decreased in diseased compared to normal tissues, the majority associated with invasive carcinoma. Some of these have already been linked with breast cancer and many affect key cellular events connected to tumorigenesis. Analysis of selected target proteins using complementary methods confirmed the changes observed with iTRAQ quantitation.

The cofilin pathway has previously been established as a key step in the invasiveness and metastasis of breast cancer[40], however our results represent the most comprehensive analysis of cofilin-1 as a possible biomarker of the disease. Our results indicated that cofilin-1 is ubiquitously expressed in breast epithelial cells. The protein was detected in all cancer and normal cell lines as well as primary breast epithelial cells. This included highly invasive and metastatic basal-like and Claudin-low phenotypes, which are predominantly defined as triple negative. Cofilin-1 activity in cell motility, which forms the initial step of invasiveness, is stimulated by EGF receptor[55]. In the absence of HER2, triple negative breast cancers may activate the cofilin pathway through other members of the EGF receptor family or independent mechanisms. The presence of cofilin-1 in some normal tissues from fibroadenoma and DCIS patients may reflect the epithelial cell content however there was also evidence of an increase in matched tumor samples. The extent to which cofilin-1 was detected in tissues is possibly due to epithelial cell content, which is lower in normal compared to tumor specimens, rather

than increased expression. Tissue microarray results, however, suggest that cofilin-1 expression correlates with tumor grade which relates to clinical outcome, establishing it as a strong candidate for further validation as a prognostic biomarker. This warrants further investigation with a larger patient cohort to determine if cofilin-1 is a biomarker of early breast cancer or an indicator of aberrant benign and malignant growth.

p23 exhibited many similar properties to cofilin-1 - detected in all cell lines (though with greater variability) and increased in invasive carcinomas compared to normal tissue (p23 was below the levels of detection in fibroadenoma and DCIS tissues using Western blotting and MRM MS). From TMA analysis, p23 was positively associated with ER status, correlating with its role as a modulator of estrogen receptor (ER)α-dependent transcriptional activity. The activities of p23 affect different targets based on sub-cellular localisation. In the cytoplasm it is part of the HSP90 complex that regulates steroid receptor ligand binding capacity, whereas in the nucleus it augments transcriptional activation activity of steroid receptors[56]. Our results indicated a direct correlation between cytoplasmic and nuclear levels as well as positive association with invasive ductal and lobular tumors. Increased expression of p23 in MCF7 cells was shown to convert them into an aggressive invasive phenotype[51]. Like cofilin-1, p23 was expressed in triple negative phenotype cell lines and has previously been shown to increase metastatic characteristics of this phenotype[57]. In these sources, p23 may be acting through non-steroid receptor mechanisms, hence further clinical validation as a breast cancer biomarker would be invaluable.

Overall, the results have indicated that proteomics analysis of matched tissues can generate a valuable subset of candidate proteins for further investigation. In addition, proteins identified with low confidence but are reproducibly detected, such as p23, accurately reflect the expression levels corroborated by complementary methods. Bioinformatics tools assisted the identification of relationships and networks between groups of proteins and identified additional targets for biomarker validation.

Acknowledgements

The authors would like to thank the Cyprus Research Promotion Foundation (grants 0406/10, 0609/04 and 0311/07), Europa Donna Cyprus and MarfinLaiki Bank for supporting this research, Yorkshire Cancer Research for the support of SuS, CS, PL, AMH and VS (BPP049 and B209PG). We are grateful to Dr Pauline Carder, Pathologist; Dr V. Makris, General Surgeon; Dr C. Oxynou and Dr I. Zouvani, Histopathologists; Dr Y. Markou, Medical Oncologist and Dr M. Daniel, Radiation Oncologist for their expertise and for helping with patient recruitment. We also thank the patients for their participation and without whom this work would not be possible. Thanks to Mike Shires at the Leeds Institute of Cancer and Pathology for preparation and analysis of TMA samples.

Supporting Information Available: This material is available free of charge via the Internet at http://pubs.acs.org.

References

1. Hery, C.; Ferlay, J.; Boniol, M.; Autier, P., Changes in breast cancer incidence and mortality in middle-aged and elderly women in 28 countries with Caucasian majority populations. *Ann Oncol* **2008,** *19* (5), 1009-18.
2. Benson, J. R.; Jatoi, I., The global breast cancer burden. *Future Oncol* **2012,** *8* (6), 697-702.
3. Herschkowitz, J. I.; Simin, K.; Weigman, V. J.; Mikaelian, I.; Usary, J.; Hu, Z.; Rasmussen, K. E.; Jones, L. P.; Assefnia, S.; Chandrasekharan, S.; Backlund, M. G.; Yin, Y.; Khramtsov, A. I.; Bastein, R.; Quackenbush, J.; Glazer, R. I.; Brown, P. H.; Green, J. E.; Kopelovich, L.; Furth, P. A.; Palazzo, J. P.; Olopade, O. I.; Bernard, P. S.; Churchill, G. A.; Van Dyke, T.; Perou, C. M., Identification of conserved gene expression features between murine mammary carcinoma models and human breast tumors. *Genome Biol* **2007,** *8* (5), R76.
4. Curtis, C.; Shah, S. P.; Chin, S. F.; Turashvili, G.; Rueda, O. M.; Dunning, M. J.; Speed, D.; Lynch, A. G.; Samarajiwa, S.; Yuan, Y.; Graf, S.; Ha, G.; Haffari, G.; Bashashati, A.; Russell, R.; McKinney, S.; Group, M.; Langerod, A.; Green, A.; Provenzano, E.; Wishart, G.; Pinder, S.; Watson, P.; Markowetz, F.; Murphy, L.; Ellis, I.; Purushotham, A.; Borresen-Dale, A. L.; Brenton, J. D.; Tavare, S.; Caldas, C.; Aparicio, S., The genomic and transcriptomic architecture of 2,000 breast tumours reveals novel subgroups. *Nature* **2012,** *486* (7403), 346-52.
5. Hanby, A. M., Aspects of molecular phenotype and its correlations with breast cancer behaviour and taxonomy. *Br J Cancer* **2005,** *92* (4), 613-7.
6. Mokbel, K., Towards optimal management of ductal carcinoma in situ of the breast. *Eur J Surg Oncol* **2003,** *29* (2), 191-7.
7. Sutton, C. W.; Rustogi, N.; Gurkan, C.; Scally, A.; Loizidou, M. A.; Hadjisavvas, A.; Kyriacou, K., Quantitative proteomic profiling of matched normal and tumor breast tissues. *J Proteome Res* **2010,** *9* (8), 3891-902.
8. Bradford, M. M., A rapid and sensitive method for the quantitation of microgram quantities of protein utilizing the principle of protein-dye binding. *Anal Biochem* **1976,** *72*, 248-54.
9. Perkins, D. N.; Pappin, D. J.; Creasy, D. M.; Cottrell, J. S., Probability-based protein identification by searching sequence databases using mass spectrometry data. *Electrophoresis* **1999,** *20* (18), 3551-67.
10. Simpkins, S. A.; Hanby, A. M.; Holliday, D. L.; Speirs, V., Clinical and functional significance of loss of caveolin-1 expression in breast cancer-associated fibroblasts. *J Pathol* **2012,** *227* (4), 490-8.
11. Collins, L. C.; Botero, M. L.; Schnitt, S. J., Bimodal frequency distribution of estrogen receptor immunohistochemical staining results in breast cancer: an analysis of 825 cases. *Am J Clin Pathol* **2005,** *123* (1), 16-20.
12. Simpson, N. E.; Lambert, W. M.; Watkins, R.; Giashuddin, S.; Huang, S. J.; Oxelmark, E.; Arju, R.; Hochman, T.; Goldberg, J. D.; Schneider, R. J.; Reiz, L. F.; Soares, F. A.; Logan, S. K.; Garabedian, M. J., High levels of Hsp90 cochaperone p23 promote tumor progression and poor prognosis in breast cancer by increasing lymph node metastases and drug resistance. *Cancer Res* **2010,** *70* (21), 8446-56.
13. Wulfkuhle, J. D.; Sgroi, D. C.; Krutzsch, H.; McLean, K.; McGarvey, K.; Knowlton, M.; Chen, S.; Shu, H.; Sahin, A.; Kurek, R.; Wallwiener, D.; Merino, M. J.; Petricoin, E. F., 3rd; Zhao, Y.; Steeg, P. S., Proteomics of human breast ductal carcinoma in situ. *Cancer Res* **2002,** *62* (22), 6740-9.
14. Kabbage, M.; Chahed, K.; Hamrita, B.; Guillier, C. L.; Trimeche, M.; Remadi, S.; Hoebeke, J.; Chouchane, L., Protein alterations in infiltrating ductal carcinomas of the breast as detected by nonequilibrium pH gradient electrophoresis and mass spectrometry. *J Biomed Biotechnol* **2008,** *2008*, 564127.
15. Celis, J. E.; Gromova, I.; Cabezon, T.; Gromov, P.; Shen, T.; Timmermans-Wielenga, V.; Rank, F.; Moreira, J. M., Identification of a subset of breast carcinomas characterized by expression of cytokeratin

15: relationship between CK15+ progenitor/amplified cells and pre-malignant lesions and invasive disease. *Mol Oncol* **2007,** *1* (3), 321-49.
16. Alix-Panabieres, C.; Vendrell, J. P.; Slijper, M.; Pelle, O.; Barbotte, E.; Mercier, G.; Jacot, W.; Fabbro, M.; Pantel, K., Full-length cytokeratin-19 is released by human tumor cells: a potential role in metastatic progression of breast cancer. *Breast Cancer Res* **2009,** *11* (3), R39.
17. Cimpean, A. M.; Suciu, C.; Ceausu, R.; Tatucu, D.; Muresan, A. M.; Raica, M., Relevance of the immunohistochemical expression of cytokeratin 8/18 for the diagnosis and classification of breast cancer. *Rom J Morphol Embryol* **2008,** *49* (4), 479-83.
18. Kongara, S.; Kravchuk, O.; Teplova, I.; Lozy, F.; Schulte, J.; Moore, D.; Barnard, N.; Neumann, C. A.; White, E.; Karantza, V., Autophagy regulates keratin 8 homeostasis in mammary epithelial cells and in breast tumors. *Mol Cancer Res* **2010,** *8* (6), 873-84.
19. Debily, M. A.; Marhomy, S. E.; Boulanger, V.; Eveno, E.; Mariage-Samson, R.; Camarca, A.; Auffray, C.; Piatier-Tonneau, D.; Imbeaud, S., A functional and regulatory network associated with PIP expression in human breast cancer. *PLoS One* **2009,** *4* (3), e4696.
20. Alexander, H.; Stegner, A. L.; Wagner-Mann, C.; Du Bois, G. C.; Alexander, S.; Sauter, E. R., Proteomic analysis to identify breast cancer biomarkers in nipple aspirate fluid. *Clin Cancer Res* **2004,** *10* (22), 7500-10.
21. Lwin, Z. M.; Guo, C.; Salim, A.; Yip, G. W.; Chew, F. T.; Nan, J.; Thike, A. A.; Tan, P. H.; Bay, B. H., Clinicopathological significance of calreticulin in breast invasive ductal carcinoma. *Mod Pathol* **2010,** *23* (12), 1559-66.
22. Lee, H. H.; Lim, C. A.; Cheong, Y. T.; Singh, M.; Gam, L. H., Comparison of protein expression profiles of different stages of lymph nodes metastasis in breast cancer. *Int J Biol Sci* **2012,** *8* (3), 353-62.
23. Miksicek, R. J.; Myal, Y.; Watson, P. H.; Walker, C.; Murphy, L. C.; Leygue, E., Identification of a novel breast- and salivary gland-specific, mucin-like gene strongly expressed in normal and tumor human mammary epithelium. *Cancer Res* **2002,** *62* (10), 2736-40.
24. Ayerbes, M. V.; Diaz-Prado, S.; Ayude, D.; Campelo, R. G.; Iglesias, P.; Haz, M.; Medina, V.; Gallegos, I.; Quindos, M.; Aparicio, L. A., In silico and in vitro analysis of small breast epithelial mucin as a marker for bone marrow micrometastasis in breast cancer. *Adv Exp Med Biol* **2008,** *617*, 331-9.
25. Tamesa, M. S.; Kuramitsu, Y.; Fujimoto, M.; Maeda, N.; Nagashima, Y.; Tanaka, T.; Yamamoto, S.; Oka, M.; Nakamura, K., Detection of autoantibodies against cyclophilin A and triosephosphate isomerase in sera from breast cancer patients by proteomic analysis. *Electrophoresis* **2009,** *30* (12), 2168-81.
26. Simpson, N. E.; Gertz, J.; Imberg, K.; Myers, R. M.; Garabedian, M. J., Research resource: enhanced genome-wide occupancy of estrogen receptor alpha by the cochaperone p23 in breast cancer cells. *Mol Endocrinol* **2012,** *26* (1), 194-202.
27. Frasor, J.; Weaver, A. E.; Pradhan, M.; Mehta, K., Synergistic up-regulation of prostaglandin E synthase expression in breast cancer cells by 17beta-estradiol and proinflammatory cytokines. *Endocrinology* **2008,** *149* (12), 6272-9.
28. Ho, J.; Kong, J. W.; Choong, L. Y.; Loh, M. C.; Toy, W.; Chong, P. K.; Wong, C. H.; Wong, C. Y.; Shah, N.; Lim, Y. P., Novel breast cancer metastasis-associated proteins. *J Proteome Res* **2009,** *8* (2), 583-94.
29. Rower, C.; Koy, C.; Hecker, M.; Reimer, T.; Gerber, B.; Thiesen, H. J.; Glocker, M. O., Mass spectrometric characterization of protein structure details refines the proteome signature for invasive ductal breast carcinoma. *J Am Soc Mass Spectrom* **2011,** *22* (3), 440-56.
30. Gromov, P.; Gromova, I.; Bunkenborg, J.; Cabezon, T.; Moreira, J. M.; Timmermans-Wielenga, V.; Roepstorff, P.; Rank, F.; Celis, J. E., Up-regulated proteins in the fluid bathing the tumour cell microenvironment as potential serological markers for early detection of cancer of the breast. *Mol Oncol* **2010,** *4* (1), 65-89.

31. Caruso, J. A.; Stemmer, P. M., Proteomic profiling of lipid rafts in a human breast cancer model of tumorigenic progression. *Clin Exp Metastasis* **2011,** *28* (6), 529-40.
32. Hancke, K.; Grubeck, D.; Hauser, N.; Kreienberg, R.; Weiss, J. M., Adipocyte fatty acid-binding protein as a novel prognostic factor in obese breast cancer patients. *Breast Cancer Res Treat* **2010,** *119* (2), 367-7.
33. Tang, X. Y.; Umemura, S.; Tsukamoto, H.; Kumaki, N.; Tokuda, Y.; Osamura, R. Y., Overexpression of fatty acid binding protein-7 correlates with basal-like subtype of breast cancer. *Pathol Res Pract* **2010,** *206* (2), 98-101.
34. Harvell, D. M.; Spoelstra, N. S.; Singh, M.; McManaman, J. L.; Finlayson, C.; Phang, T.; Trapp, S.; Hunter, L.; Dye, W. W.; Borges, V. F.; Elias, A.; Horwitz, K. B.; Richer, J. K., Molecular signatures of neoadjuvant endocrine therapy for breast cancer: characteristics of response or intrinsic resistance. *Breast Cancer Res Treat* **2008,** *112* (3), 475-88.
35. Davalos, A.; Fernandez-Hernando, C.; Sowa, G.; Derakhshan, B.; Lin, M. I.; Lee, J. Y.; Zhao, H.; Luo, R.; Colangelo, C.; Sessa, W. C., Quantitative proteomics of caveolin-1-regulated proteins: characterization of polymerase i and transcript release factor/CAVIN-1 IN endothelial cells. *Mol Cell Proteomics* **2010,** *9* (10), 2109-24.
36. Guerin, M.; Barrois, M.; Terrier, M. J.; Spielmann, M.; Riou, G., Overexpression of either c-myc or c-erbB-2/neu proto-oncogenes in human breast carcinomas: correlation with poor prognosis. *Oncogene Res* **1988,** *3* (1), 21-31.
37. Wang, G.; Platt-Higgins, A.; Carroll, J.; de Silva Rudland, S.; Winstanley, J.; Barraclough, R.; Rudland, P. S., Induction of metastasis by S100P in a rat mammary model and its association with poor survival of breast cancer patients. *Cancer Res* **2006,** *66* (2), 1199-207.
38. Yuan, Y.; Nymoen, D. A.; Dong, H. P.; Bjorang, O.; Shih Ie, M.; Low, P. S.; Trope, C. G.; Davidson, B., Expression of the folate receptor genes FOLR1 and FOLR3 differentiates ovarian carcinoma from breast carcinoma and malignant mesothelioma in serous effusions. *Hum Pathol* **2009,** *40* (10), 1453-60.
39. Shatz, M.; Liscovitch, M., Caveolin-1: a tumor-promoting role in human cancer. *Int J Radiat Biol* **2008,** *84* (3), 177-89.
40. Wang, W.; Eddy, R.; Condeelis, J., The cofilin pathway in breast cancer invasion and metastasis. *Nat Rev Cancer* **2007,** *7* (6), 429-40.
41. Wang, W. S.; Zhong, H. J.; Xiao, D. W.; Huang, X.; Liao, L. D.; Xie, Z. F.; Xu, X. E.; Shen, Z. Y.; Xu, L. Y.; Li, E. M., The expression of CFL1 and N-WASP in esophageal squamous cell carcinoma and its correlation with clinicopathological features. *Dis Esophagus* **2010,** *23* (6), 512-21.
42. Yang, Z. L.; Miao, X.; Xiong, L.; Zou, Q.; Yuan, Y.; Li, J.; Liang, L.; Chen, M.; Chen, S., CFL1 and Arp3 are biomarkers for metastasis and poor prognosis of squamous cell/adenosquamous carcinomas and adenocarcinomas of gallbladder. *Cancer Invest* **2013,** *31* (2), 132-9.
43. Zhou, J.; Wang, Y.; Fei, J.; Zhang, W., Expression of cofilin 1 is positively correlated with the differentiation of human epithelial ovarian cancer. *Oncol Lett* **2012,** *4* (6), 1187-1190.
44. Nishimura, S.; Tsuda, H.; Kataoka, F.; Arao, T.; Nomura, H.; Chiyoda, T.; Susumu, N.; Nishio, K.; Aoki, D., Overexpression of cofilin 1 can predict progression-free survival in patients with epithelial ovarian cancer receiving standard therapy. *Hum Pathol* **2011,** *42* (4), 516-21.
45. Muller, C. B.; de Barros, R. L.; Castro, M. A.; Lopes, F. M.; Meurer, R. T.; Roehe, A.; Mazzini, G.; Ulbrich-Kulczynski, J. M.; Dal-Pizzol, F.; Fernandes, M. C.; Moreira, J. C.; Xavier, L. L.; Klamt, F., Validation of cofilin-1 as a biomarker in non-small cell lung cancer: application of quantitative method in a retrospective cohort. *J Cancer Res Clin Oncol* **2011,** *137* (9), 1309-16.
46. Castro, M. A.; Dal-Pizzol, F.; Zdanov, S.; Soares, M.; Muller, C. B.; Lopes, F. M.; Zanotto-Filho, A.; da Cruz Fernandes, M.; Moreira, J. C.; Shacter, E.; Klamt, F., CFL1 expression levels as a prognostic and drug resistance marker in nonsmall cell lung cancer. *Cancer* **2010,** *116* (15), 3645-55.

47. Turhani, D.; Krapfenbauer, K.; Thurnher, D.; Langen, H.; Fountoulakis, M., Identification of differentially expressed, tumor-associated proteins in oral squamous cell carcinoma by proteomic analysis. *Electrophoresis* **2006,** *27* (7), 1417-23.
48. Wang, Y.; Kuramitsu, Y.; Ueno, T.; Suzuki, N.; Yoshino, S.; Iizuka, N.; Zhang, X.; Oka, M.; Nakamura, K., Differential expression of up-regulated cofilin-1 and down-regulated cofilin-2 characteristic of pancreatic cancer tissues. *Oncol Rep* **2011,** *26* (6), 1595-9.
49. Unwin, R. D.; Craven, R. A.; Harnden, P.; Hanrahan, S.; Totty, N.; Knowles, M.; Eardley, I.; Selby, P. J.; Banks, R. E., Proteomic changes in renal cancer and co-ordinate demonstration of both the glycolytic and mitochondrial aspects of the Warburg effect. *Proteomics* **2003,** *3* (8), 1620-32.
50. Sullivan, W.; Stensgard, B.; Caucutt, G.; Bartha, B.; McMahon, N.; Alnemri, E. S.; Litwack, G.; Toft, D., Nucleotides and two functional states of hsp90. *J Biol Chem* **1997,** *272* (12), 8007-12.
51. Oxelmark, E.; Roth, J. M.; Brooks, P. C.; Braunstein, S. E.; Schneider, R. J.; Garabedian, M. J., The cochaperone p23 differentially regulates estrogen receptor target genes and promotes tumor cell adhesion and invasion. *Mol Cell Biol* **2006,** *26* (14), 5205-13.
52. Toogun, O. A.; Dezwaan, D. C.; Freeman, B. C., The hsp90 molecular chaperone modulates multiple telomerase activities. *Mol Cell Biol* **2008,** *28* (1), 457-67.
53. Tanioka, T.; Nakatani, Y.; Kobayashi, T.; Tsujimoto, M.; Oh-ishi, S.; Murakami, M.; Kudo, I., Regulation of cytosolic prostaglandin E2 synthase by 90-kDa heat shock protein. *Biochem Biophys Res Commun* **2003,** *303* (4), 1018-23.
54. Toninello, A.; Pietrangeli, P.; De Marchi, U.; Salvi, M.; Mondovi, B., Amine oxidases in apoptosis and cancer. *Biochimica et biophysica acta* **2006,** *1765* (1), 1-13.
55. Song, X.; Chen, X.; Yamaguchi, H.; Mouneimne, G.; Condeelis, J. S.; Eddy, R. J., Initiation of cofilin activity in response to EGF is uncoupled from cofilin phosphorylation and dephosphorylation in carcinoma cells. *J Cell Sci* **2006,** *119* (Pt 14), 2871-81.
56. Reebye, V.; Querol Cano, L.; Lavery, D. N.; Brooke, G. N.; Powell, S. M.; Chotai, D.; Walker, M. M.; Whitaker, H. C.; Wait, R.; Hurst, H. C.; Bevan, C. L., Role of the HSP90-associated cochaperone p23 in enhancing activity of the androgen receptor and significance for prostate cancer. *Mol Endocrinol* **2012,** *26* (10), 1694-706.
57. Goldblatt, E. M.; Gentry, E. R.; Fox, M. J.; Gryaznov, S. M.; Shen, C.; Herbert, B. S., The telomerase template antagonist GRN163L alters MDA-MB-231 breast cancer cell morphology, inhibits growth, and augments the effects of paclitaxel. *Mol Cancer Ther* **2009,** *8* (7), 2027-35.

Figure Legends

Figure 1. (A). Venn diagram showing the association of proteins identified in three iTRAQ experiments A, B and C. (B). Cluster analysis for the 402 proteins identified in all three experiments with tumor:normal iTRAQ ratios for each protein for each patient represented as upper 25 percentile (green), lower 25 percentile (red) or unchanged (yellow), and ordered by the average iTRAQ ratio for the invasive carcinoma patients.

Figure 2. Protein-protein interactions determined by STRING analysis for the increased (green border), decreased (red border) and associated unaffected proteins (amber border) in tumor compared to normal tissues (Table 2). Thicker lines represent stronger confidence of association between proteins. Proteins associated with redox equilibrium (A), lipid transport/metabolism (B), protein folding (C), cell assembly, morphology and organisation (D) and mitochondrial localisation (E) are clustered together (------).

Figure 3. Western blot analysis (A) cofilin-1, p23, AOC3 and β-actin expression in matched normal and tumor tissues of four invasive carcinoma patients, (B) cofilin-1 expression in matched normal and tumor tissues of fibroadenoma and DCIS patients,

Figure 4. MRM MS – breast cancer patent tissues - concentrations of cofilin-1 (A), p23 (B) and AOC3 (C) in amol/mg of tissue

Figures

Figure 1

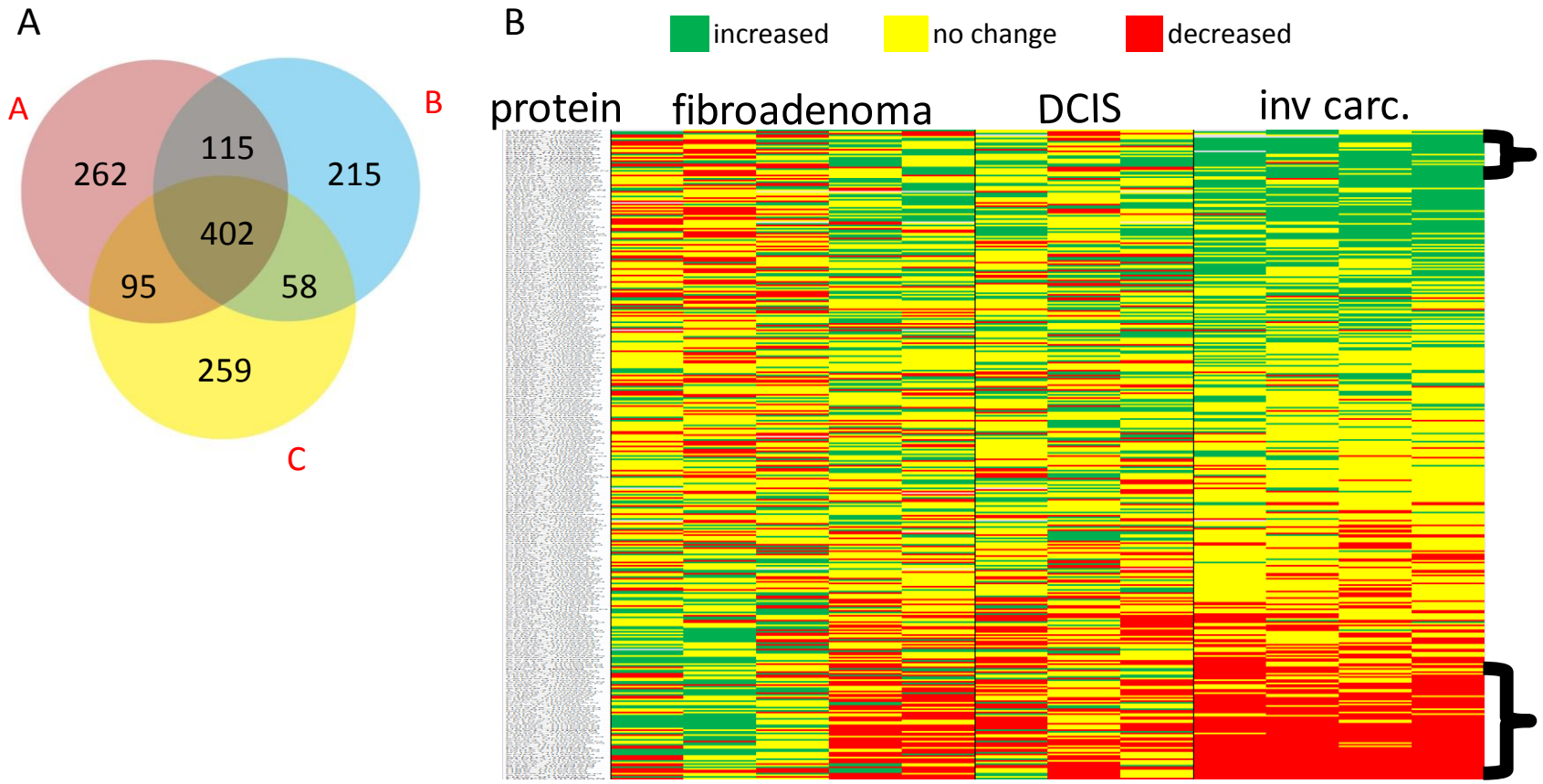

Figure 2

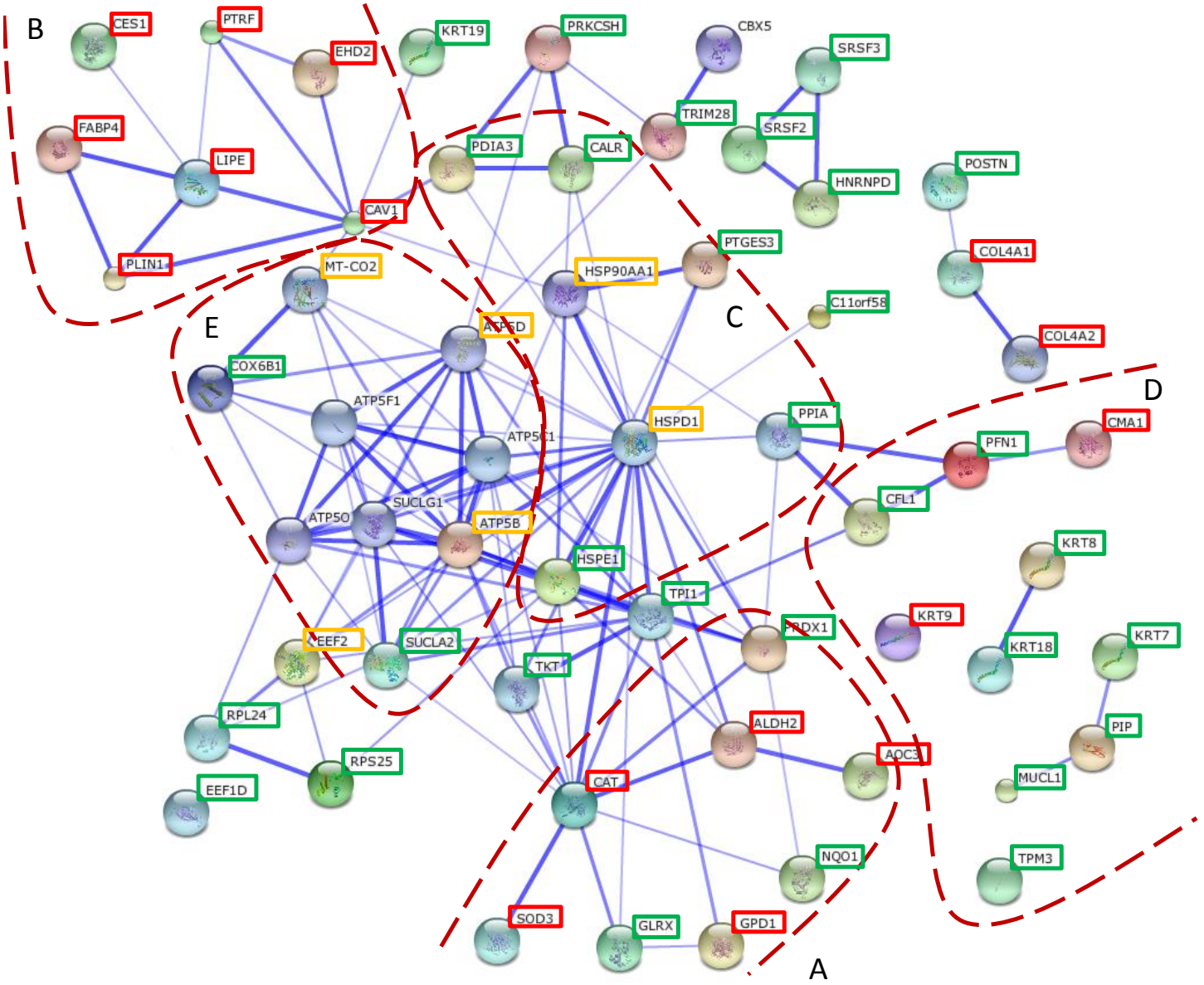
B
CES1
PTRF
EHD2
KRT19
PRKCSH
CBX5
SRSF3
FABP4
LIPE
PDIA3
CALR
TRIM28
SRSF2
HNRNPD
POSTN
CAV1
PLIN1
MT-CO2
HSP90AA1
PTGES3
COL4A1
C11orf58
E
C
ATP5D
COX6B1
COL4A2
D
ATP5F1
HSPD1
PPIA
CMA1
ATP5C1
PFN1
CFL1
SUCLG1
ATP5O
ATP5B
KRT8
HSPE1
TPI1
KRT9
PRDX1
KRT18
KRT7
EEF2
SUCLA2
TKT
RPL24
ALDH2
AOC3
PIP
RPS25
CAT
MUCL1
EEF1D
NQO1
TPM3
SOD3
GLRX
GPD1
A

Figure 3

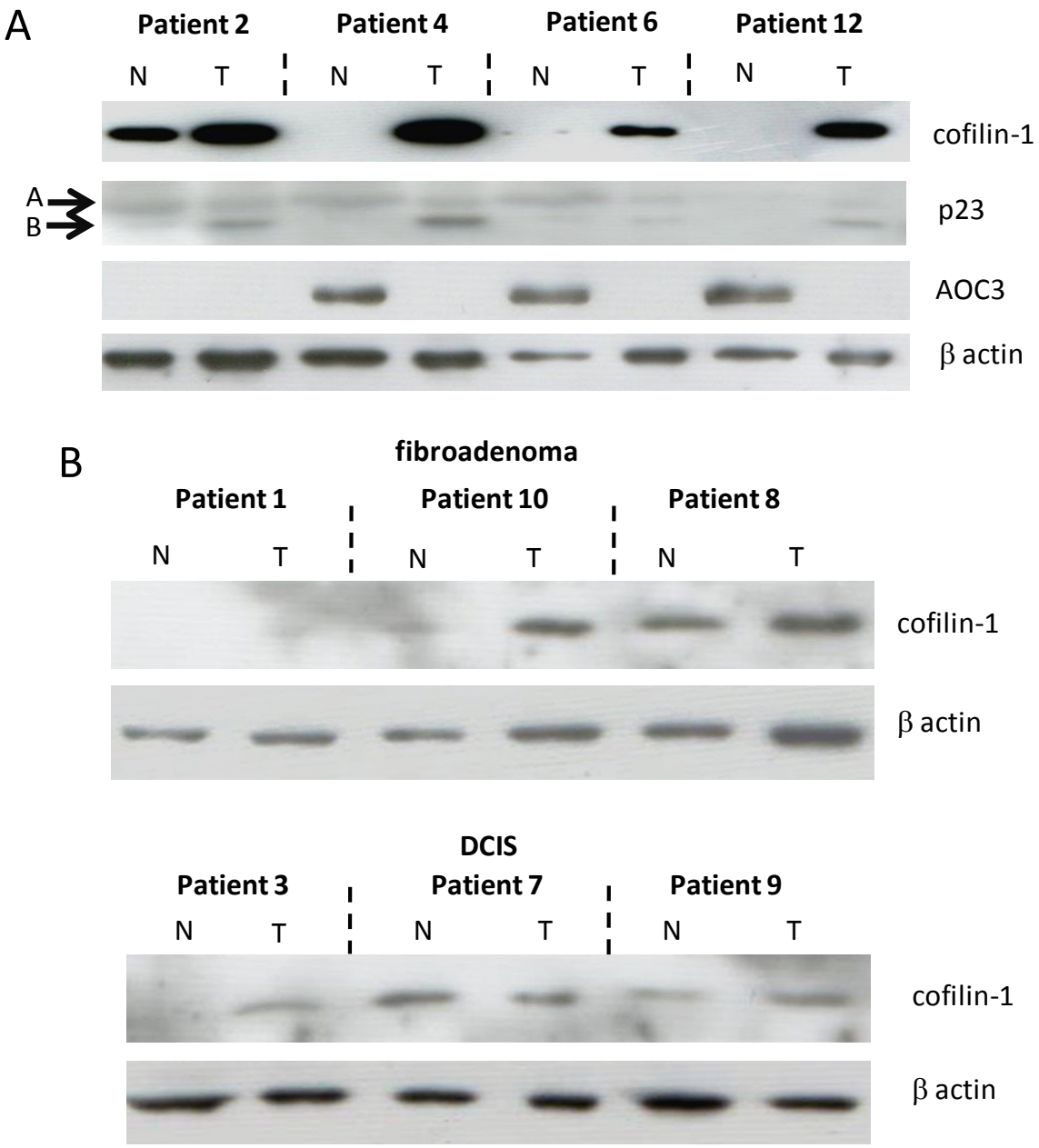
A
Patient 2
Patient 4
Patient 6
Patient 12
N
T
cofilin-1
A
B
p23
AOC3
β actin
B
fibroadenoma
Patient 1
Patient 10
Patient 8
cofilin-1
β actin
DCIS
Patient 3
Patient 7
Patient 9
cofilin-1
β actin

Figure 4

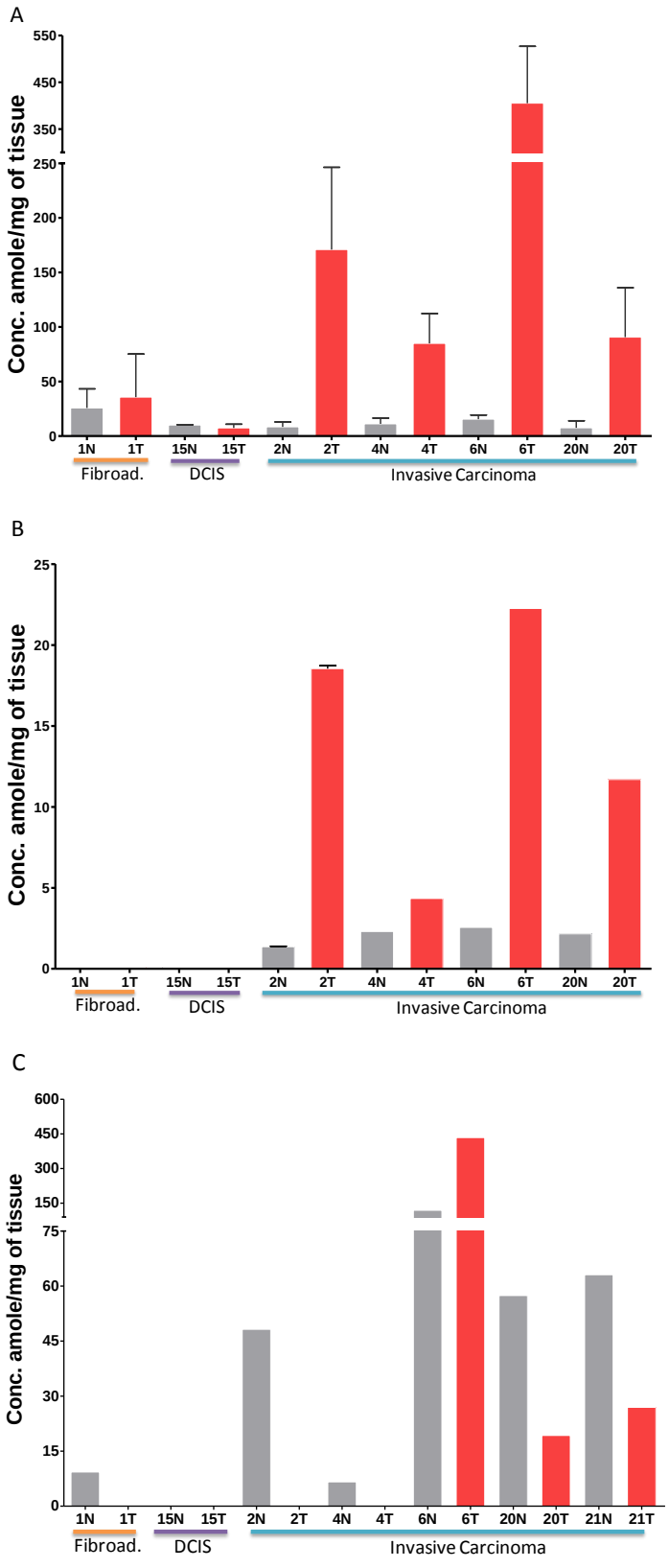
A
Conc. amole/mg of tissue
550
450
350
250
200
150
100
50
0
1N 1T 15N 15T 2N 2T 4N 4T 6N 6T 20N 20T
Fibroad.
DCIS
Invasive Carcinoma
B
Conc. amole/mg of tissue
25
20
15
10
5
0
1N 1T 15N 15T 2N 2T 4N 4T 6N 6T 20N 20T
Fibroad.
DCIS
Invasive Carcinoma
C
Conc. amole/mg of tissue
600
450
300
150
75
60
45
30
15
0
1N 1T 15N 15T 2N 2T 4N 4T 6N 6T 20N 20T 21N 21T
Fibroad.
DCIS
Invasive Carcinoma

Tables

Table 1. Details of patients 1 to 10 including histopathology grade, age, tumor size, ER, PR and L/N status and iTRAQ reagent.

Table 2. Summary of the significant up- and down-regulated proteins. Significant proteins were defined at those with tumor-to-normal ratios in the upper or lower 5% or 10% of the total (402 common proteins), for at least 3 of 5 fibroadenoma, 2 of 3 DCIS or 3 of 4 invasive carcinoma patients and in the upper or lower 25% for at least 4 of 5 fibroadenoma, 3 of 3 DCIS or 4 of 4 invasive carcinoma patients. u = up-regulated and d = down-regulated proteins in tumor compared to normal breast tissue.

Table 3. Immunohistochemical detection correlated to the clinicopathological features of the TMA cohort. A. cofilin-1 and B. p23

Table 1. Details of Cyprus patients 1 to 10 including histopathology grade, age, tumor size, ER, PR and L/N status and iTRAQ reagent.

	Patient	Histopathology	Grade	Age	Lesion cm	Menopause	ER	PgR	L/N status	iTRAQ label T/N
Experiment 1	patient 3	DCIS	high	46	1.5	pre	-	-	0/2 +ve	114/113
	patient 5	invasive ductal carcinoma	ND	50	3.0	pre	+	+	9/22 +ve	116/115
	patient 4	invasive ductal carcinoma	II	80	4.0	post	+	-	17/23 +ve	118/117
	patient 1	fibroadenoma	N/A	24	4.0	pre	+	+	N/A	121/119
Experiment 2	patient 1	fibroadenoma	N/A	24	4.0	pre	+	+	N/A	114/113
	patient 6	invasive ductal carcinoma	I	53	2.0	post	+	+	0/4 +ve	116/115
	patient 2	invasive ductal carcinoma	III	76	3.5	post	-	-	6/9 +ve	118/117
	patient 7	DCIS	high	64	1.8	post	-	-	1 +ve	121/119
Experiment 3	patient 9	DCIS	low	76	3.0	post	-	-	0/10	114/113
	patient 8	fibroadenoma	N/A	45	2.5	pre	+	+	N/A	116/115
	patient 1	fibroadenoma	N/A	24	4.0	pre	+	+	N/A	118/117
	patient 10	fibroadenoma	N/A	27	2.0	pre	+	+	N/A	121/119

ND = not determined
N/A = not applicable

Table 2. Summary of the significant up- and down-regulated proteins in IC and DCIS

Accession	Gene	Protein	MW [kDa]	pI	ave score	ave #	ave SC	ave IC ratio	ad. 5%	ad. 10%	ad. 25%	DCIS 5%	DCIS 10%	DCIS 25%	IC 5%	IC 10%	IC 25%
TEBP_HUMAN	PGTES3	Prostaglandin E synthase 3, p23	18.7	4.2	31	1	9	2.161							3/4 u	3/4 u	3/4 u
TIF1B_HUMAN	TRIM28	Transcription intermediary factor 1-beta	88.5	5.4	71	2	4	1.841				2/3 u	2/3 u	2/3 u	2/4 u	2/4 u	3/4 u
SMAP_HUMAN	C11orf58	Small acidic protein	20.3	4.4	51	1	5	1.840						2/3 u	3/4 u	3/4 u	4/4 u
RL24_HUMAN	RPL24	60S ribosomal protein L24	17.8	12.0	91	3	16	1.840							2/4 u	3/4 u	3/4 u
COF1_HUMAN	CFL1	Cofilin-1	18.5	9.1	462	10	42	1.836							2/4 u	3/4 u	4/4 u
SFRS3_HUMAN	SRSF3	Splicing factor, arginine/serine-rich 3	19.3	12.3	88	3	17	1.835	3/5 u								4/4 u
CRIP1_HUMAN	CRIP1	Cysteine-rich protein 1	8.5	10.2	82	3	31	1.786						2/3 d	2/4 u	3/4 u	3/4 u
SH3L1_HUMAN	SH3BGRL	SH3 domain-binding glutamic acid-rich-like protein	12.8	5.1	157	3	31	1.772							2/4 u	3/4 u	4/4 u
CX6B1_HUMAN	COX6B1	Cytochrome c oxidase subunit VIb isoform 1	10.2	7.5	80	2	22	1.732	3/5 u	4/5 u							
PPIA_HUMAN	PPIA	Peptidyl-prolyl cis-trans isomerase A	18.0	9.0	835	16	69	1.703							2/4 u	4/4 u	4/4 u
K1C19_HUMAN	KRT19	Keratin, type I cytoskeletal 19	44.1	4.9	1352	29	57	1.665						2/3 u	2/4 u	3/4 u	4/4 u
CH10_HUMAN	HSPE1	10 kDa heat shock protein, mito.	10.9	9.4	232	5	45	1.657							3/4 u	3/4 u	3/4 u
K2C8_HUMAN	KRT8	Keratin, type II cytoskeletal 8	53.7	5.4	1117	24	43	1.639					2/3 u	3/3 u		3/4 u	3/4 u
MUCL_HUMAN	MUCL1	Small breast epithelial mucin	9.0	4.2	47	2	9	1.630						2/3 u	3/4 u	3/4 u	3/4 u
CALR_HUMAN	CALR	Calreticulin	48.1	4.1	353	10	24	1.614									4/4 u
SFRS2_HUMAN	SRFS2	Splicing factor, arginine/serine-rich 2	25.5	12.4	65	2	6	1.591						2/3 u	2/4 u	2/4 u	3/4 u
GLRX1_HUMAN	GLRX	Glutaredoxin-1	11.8	9.7	64	2	23	1.584					2/3 d	2/3 d	2/4 u	3/4 u	3/4 u
HMGN2_HUMAN	HMGN2	Nonhistone chromosomal protein HMG-17	9.4	10.5	103	3	30	1.557							2/4 u	2/4 u	3/4 u
EF1D_HUMAN	EEF1D	Elongation factor 1-delta	31.1	4.8	223	6	18	1.554									4/4 u
GLU2B_HUMAN	PRKCSH	Glucosidase 2 subunit beta	59.4	4.2	186	7	10	1.549								3/4 u	4/4 u
PRDX1_HUMAN	PRDX1	Peroxiredoxin-1	22.1	9.2	657	13	52	1.532							2/4 u	2/4 u	3/4 u
H2A1H_HUMAN	HIST1H2AH	Histone H2A type 1-H	13.9	11.3	459	9	47	1.513						2/3 u			4/4 u
TPIS_HUMAN	TPI1	Triosephosphate isomerase	26.7	6.5	858	15	63	1.452									4/4 u
HNRPD_HUMAN	HNRNPD	Heterogeneous nuclear ribonucleoprotein D0	38.4	8.5	235	6	15	1.443									4/4 u
PROF1_HUMAN	PFN1	Profilin-1	15.0	9.4	691	11	57	1.402									4/4 u
K2C7_HUMAN	KRT7	Keratin, type II cytoskeletal 7	51.4	5.4	1158	23	44	1.398					2/3 u	3/3 u			4/4 u
TPM3_HUMAN	TPM3	Tropomyosin alpha-3 chain	32.8	4.5	557	16	36	1.387									4/4 u
PDIA3_HUMAN	PDIA3	Protein disulfide-isomerase A3	56.7	5.9	817	21	37	1.383									4/4 u
ACBP_HUMAN	DBI	Acyl-CoA-binding protein	10.0	6.2	267	6	66	1.367						3/3 u			3/4 u
RS25_HUMAN	RPS25	40S ribosomal protein S25	13.7	10.6	28	1	6	1.341				2/3 u	2/3 u	3/3 u			
DSCAM_HUMAN	DSCAM	Down syndrome cell adhesion molecule	222.1	8.5	62	3	2	1.259				2/3 u	2/3 u	2/3 u			
K1C18_HUMAN	KRT18	Keratin, type I cytoskeletal 18	48.0	5.2	581	17	29	1.197					2/3 u	3/3 u			3/4 u
EF2_HUMAN	EEF2	Elongation factor 2	95.3	6.4	264	7	11	1.035			4/5 d						
TKT_HUMAN	TKT	Transketolase	67.8	8.5	182	6	9	0.826						3/3 u			
NQO1_HUMAN	NQ01	NAD(P)H dehydrogenase	30.8	9.4	47	1	6	0.809				2/3 u	2/3 u	2/3 u			
ATPB_HUMAN	ATP5B	ATP synthase subunit beta, mito.	56.5	5.1	411	11	26	0.805					2/3 u	3/3 u			
COR1C_HUMAN	CORO1C	Coronin-1C	53.2	6.7	39	1	3	0.772		4/5 d							
CMA1_HUMAN	CMA1	Chymase	27.3	10.4	435	8	32	0.711						3/3 d			
K1C9_HUMAN	KRT9	Keratin, type I cytoskeletal 9	62.1	5.1	253	8	13	0.679				2/3 d	2/3 d	3/3 d			
CLM1_HUMAN	CD300LF	CMRF35-like-molecule 1	32.3	5.5	27	1	4	0.647					3/3 d	3/3 d			
PIP_HUMAN	PIP	Prolactin-inducible protein	16.6	9.3	285	6	45	0.590				2/3 u	2/3 u	3/3 u			3/4 d
EHD2_HUMAN	EHD2	EH domain-containing protein 2	61.1	6.0	261	8	16	0.546									4/4 d
DPYL2_HUMAN	DPYSL2	Dihydropyrimidinase-related protein	62.3	5.9	124	3	5	0.544						2/3 u			4/4 d
CAV1_HUMAN	CAV1	Caveolin-1	20.5	5.6	128	3	18	0.489			4/5 d			2/3 d			4/4 d
LAMB2_HUMAN	LAMB2	Laminin subunit beta-2	196.0	6.1	170	6	5	0.474									4/4 d
CO4A1_HUMAN	COL4A1	Collagen alpha-1(IV) chain	160.5	9.4	196	5	5	0.464									4/4 d
EST1_HUMAN	CES1	Liver carboxylesterase 1	62.5	6.2	79	3	5	0.426								3/4 d	4/4 d
SODE_HUMAN	SOD3	Extracellular superoxide dismutase [Cu-Zn]	25.8	6.2	231	5	23	0.420									4/4 d
PLIN_HUMAN	PLIN1	Perilipin	55.9	6.0	529	11	29	0.416					3/3 u	3/3 u	2/4 d	2/4 d	4/4 d
FHL1_HUMAN	FHL1	Four and a half LIM domains protein 1	36.2	10.5	194	6	16	0.405								3/4 d	4/4 d
SUCB1_HUMAN	SUCLA2	Succinyl-CoA ligase [ADP-forming] beta-chain, mito.	50.3	7.7	81	1	2	0.403								3/4 d	4/4 d
PTRF_HUMAN	PTRF	Polymerase I and transcript release factor	43.4	5.4	389	11	22	0.402						2/3 d	2/4 d	3/4 d	4/4 d
ALDH2_HUMAN	ALDH2	Aldehyde dehydrogenase, mitochondrial	56.3	6.8	117	4	7	0.401							2/4 d	3/4 d	4/4 d
GPDA_HUMAN	GPD1	Glycerol-3-phosphate dehydrogenase [NAD+], cyto.	37.5	5.8	200	5	19	0.399							2/4 d	3/4 d	4/4 d
CATA_HUMAN	CAT	Catalase	59.7	7.0	297	7	17	0.399							2/4 d	3/4 d	4/4 d
CRYAB_HUMAN	CRYAB	Alpha crystallin B chain	20.1	6.9	89	3	16	0.327							3/4 d	4/4 d	4/4 d
AOC3_HUMAN	AOC3	Membrane copper amine oxidase	84.6	6.1	272	9	10	0.308							3/4 d	4/4 d	4/4 d
LIPS_HUMAN	LIPE	Hormone-sensitive lipase	116.5	6.2	49	1	2	0.287							3/4 d	4/4 d	4/4 d
FABPA_HUMAN	FABP4	Fatty acid-binding protein, adipocyte	14.7	7.5	349	6	41	0.256						2/3 d	4/4 d	4/4 d	4/4 d

Table 3. Immunohistochemical detection correlated to the clinicopathological features of the TMA cohort. A. cofilin-1 and B. p23

A

Characteristic	0&1 (60)	2&3(263)	p value[a]
Age Years			
Mean ±SD	55±14.82	59±14.19	0.2
Proportion Scoring			<0.0001
0	5	0	
1+	5	0	
2+	17	1	
3+	18	7	
4+	15	53	
5+	0	202	
Grade			0.03
I	20	54	
II	26	108	
III	14	101	
Type			0.003
Invasive Ductal	41	217	
Invasive Lobular	8	22	
Other	11	24	
Lymph Node Status			0.9b
No	26	112	
N1-3	31	137	
No Node taken	3	14	
ER Status			0.8
Positive	46	225	
Negative	10	46	
Tumour size (mm)			0.7
≤10	8	30	
>10	51	226	
Metastasis			0.4
0	29	149	
1	12	44	

B

Characteristic	1+(24)	2+(150)	3+(131)	1+vs2+vs3+[b]
Age Years				
Mean ±SD	62±12.12	60±14.6	57±14.13	0.5
Nuclear p23				<0.0001
0	1	0	0	
1+	12	1	0	
2+	8	20	0	
3+	3	129	131	
Grade				0.3
I	8	29	33	
II	7	72	50	
III	9	49	48	
Type				<0.0001
Invasive Ductal	14	122	106	
Invasive Lobular	2	17	11	
Other	8	11	14	
Lymph Node Status				0.6
No	9	70	56	
N1-3	12	71	71	
No Node taken	3	9	4	
ER Status				0.01
Positive	14	113	112	
Negative	7	28	17	
Tumour size (mm)				0.4
≤10	1	17	17	
>10	23	127	112	
Metastasis				0.07
0	10	85	72	
1	7	18	25	

a - p was determined by Fisher test for cofilin-1 characteristics except age for which t test was used

b - p was determined by One way ANOVA for p23 characteristics except age for which t test was used

Synopsis

As part of an initiative to identify early indicators of breast cancer, quantitative proteomics was performed on matched normal and tumor tissues from stage-specific breast cancer patients identifying 59 proteins that were significantly changed. The proteins were associated with cell morphology, cellular assembly and organisation, free radical scavenging and cell-to-cell signalling. The results were corroborated by Western blotting and MRM MS of cofilin-1 and p23, both increased, and AOC3, decreased in tumor compared to normal tissue. Widespread expression of cofilin-1 and p23 in an invasive carcinoma-centric tissue microarray analysis further validated these candidates as potential biomarkers of breast cancer.

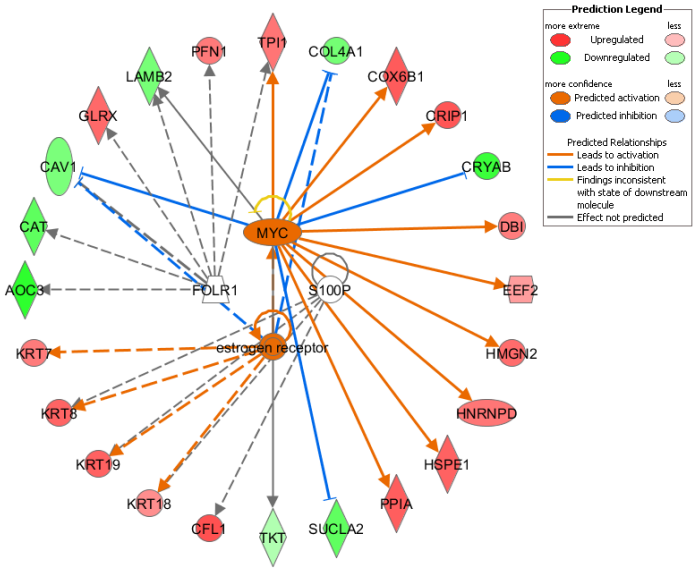

Significance

Despite strong progress in the treatment of breast cancer, the incidence of disease continues to increase. There still remains no molecular diagnostic for the early detection of breast cancer. By studying proteomics changes in matched normal and benign or malignant tumor tissues from patients with different stages of the disease, our objective was to identify candidate biomarkers for clinical validation.

Supporting Information.

Supplementary Tables

Supplementary Table 1, MRM MS - proteotypic peptide properties

Supplementary Table 2, summary of the quantitative proteomic analysis of 402 proteins identified in all three experiments. For each protein, the SwissProt accession number, name, theoretical molecular weight and pI and for each protein in each experiment (A, B and C), Mascot scores, number of peptides, sequence coverage (SC) are provided. In addition, for each protein in each experiment, for each patient, normalised median ratio, the number of iTRAQ measurements (#), and CV(%) are included.

Supplementary Figures

1. Proteomics workflow
2. MRM MS - calibration curves for proteotypic peptide standards
3. Principle component analysis of 12 iTRAQ proteomics datasets for 10 patients
4. Upstream regulator analysis for significantly increased and decreased proteins associated
5. Network analysis for significantly increased and decreased proteins associated with cell morphology, cellular assembly and organisation (a), free radical scavenging (b) and cell-to-cell signalling (c)
6. Western blot analysis of cofilin-1, p23, AOC3 and b-actin expression in (A) breast cancer cell lines of defined phenotype, (B) MCF-7 breast cancer cell line (included as a reference) normal breast cell lines and (1^{o}) primary cells. Bands marked A and B identify the 22.6kDa and 20.5kDa p23 proteins respectively.
7. MRM MS – breast cancer cell lines with concentrations of cofilin-1 (A) and p23 (B) in amol/cell
8. Representative IHC images for cofilin-1 staining, (i) strong expression (proportion score = 5, intensity score = 3) and (ii) no expression (proportion score = 0, intensity score = 0), and p23 staining, (iii) strong nuclear score of 3 and strong cytoplasmic expression score of 3, and (iv) negative nuclear score of 0 and weak cytoplasmic expression score of 1.